Effects of Temperature and Additives on NO$_x$ Emission From Combustion of Fast-Growing Grass

Haili Liu[1], Qingchao Hong[1], Heyun Liu[1], Zhen Huang[2]*, Xu Zhang[1], Wang Chen[1], Xi Zeng[1] and Shulin Pan[1]

[1]School of Energy and Mechanical Engineering, Hunan Institute of Humanities, Science and Technology, Loudi, China, [2]Guangzhou Institute of Energy Conversion, Chinese Academy of Sciences, Guangzhou, China

Fast-growing grass, as a popular renewable energy, is low in sulfur content, so NO$_x$ is the major pollutant during its combustion. To study the emission characteristics of NO$_x$ and obtain the data of controlling NO$_x$ emission, the effects of combustion temperature as well as the additive type and mass fraction were investigated on the emission characteristics of NO$_x$ from the combustion of fast-growing grass. Results revealed that the first peak for NO$_x$ emission from this combustion gradually increases with an increase in temperature. Moreover, the additives were found to dramatically impact the amount of NO$_x$ emission and its representative peak. The optimal additives and their optimal mass fractions were determined at various specific temperatures to reduce NO$_x$ emission. At combustion temperatures of 600, 700, 750, 800, and 850°C, the optimal conditions to limit NO$_x$ emissions were 5% SiO$_2$, 3% Al$_2$O$_3$, 3% Ca(OH)$_2$, 15% Al$_2$O$_3$, and 3% SiO$_2$ (or 3% Al$_2$O$_3$), respectively; the corresponding emission peaks decreased by 43.59, 44.21, 47.99, 24.18, and 30.60% (or 31.51%), with denitration rates of 63.28, 50.34, 57.44, 27.05, and 27.34% (or 27.28%), respectively.

Keywords: fast-growing grass, NOx emissions, denitration rate, emission peak, the optimal mass fraction

INTRODUCTION

Scientific and technological advances along with evolving industrialization, have been continuously improving people's living standards. However, energy consumption for this industrial development has had its own drawbacks, with the extensive use of traditional fossil fuels leading to serious environmental problems, such as air pollution and global warming. Consumption of coal, petroleum, and other traditional energy sources produces lots of SO$_2$ and NO$_x$ that eventually cause acid rain, thereby corroding houses, bridges and other constructions. Meanwhile, the emitted NO$_x$ increases the content of fine particulate matters (PM2.5) in the atmosphere. The environmental monitoring data in China has revealed that the nitrate content has exceeded the sulfate content in some cities. For instance at the Beijing-Tianjin-Hebei Urban Agglomeration, the absolute concentration and proportion of nitrate exceeded those of sulfate by a large margin during the summers between 2017 and 2018, making it the leading secondary inorganic component in PM2.5 (National Joint Center for air pollution control, 2019). Xu et al. (2019) measured water-soluble inorganic ions (WSI) in PM2.5 in Beijing between February 5 and November 15, 2017. The results showed that nitrate was the major component of WSI in PM2.5 that exacerbated the rapid growth of PM2.5 concentrations in the Fangshan District during heavy pollution. Therefore, more efforts are required to reduce NO$_x$ emission.

Developing clean and efficient renewable energy sources are urgently required. Biomass fuels are considered the best renewable organic alternative to fossil fuels because of their extremely low sulfur content and renewable characteristics (Recalde et al., 2019; Wang et al., 2021). Lvxin fast-growing grass (hereafter referred to as the "fast-growing grass") is a fast-growing plant developed by Prof. Lei Xuejun (Lei, 2015) by hybridizing seven different varieties Lvxin grass. This fast-growing grass requires intensive farming yielding wide leaves with a shape similar to sugarcane and sorghum, a height of up to 4–5 m, diameters up to 50–60 mm, and a normal yield of 5–8 tons of dried grass per mu (1 mu = 0.0667 ha). This fast-growing grass is not only resistant to high temperatures and drought, but also resilient and easy to grow. Most importantly, it can absorb heavy metal ions which makes it suitable to be applied for the remediation of heavy metal-contaminated soil (Lei, 2017). Among its various uses, an important one is as a fuel for biomass power plants. However, characteristics of NO_x emission from the combustion of this fast-growing grass have not been publicly reported.

Extensive research has demonstrated the benefits of oxides, alkali salt, and other additives on NO_x removal from biomass combustion products (RotaZanoelo, 2003; Lee et al., 2005; Sun et al., 2019; Wang et al., 2020; Xiaorui et al., 2021). Many studies have also been conducted on the wet denitration reaction along with additives (Bae et al., 2006; Niu et al., 2010; Gasnot et al., 2011; Wang et al., 2014). Hao (Hao et al., 2015) revealed a significantly positive influence of Na/K additives on the reduction of NO (with the following order: Na_2CO_3 > KCl > NaCl), which also expanded the temperature range of the elective non-catalytic reduction (SNCR) process. Cai et al. (2021) showed that adding hydrogen peroxide, sodium carbonate, ethanol, and other additives to urea-based SNCR increases the OH groups, thereby enhancing the NOx removal efficiency and widening the SNCR "temperature window". Chen et al. (2016) showed that adding urea to hydrazine hydrate solution promotes hydrazine decomposition and produces NO-reducing H free radical, thereby achieving NO_x removal. Qi (QiGe et al., 2020) demonstrated NO_x removal by gradually oxidizing NO to HNO_3 in an atmosphere of H_2O_2, OH, and HO_2 using an additive-aided H_2O_2 solution and denitration process. Incorporating additives during the combustion process is simple, convenient, cost-efficient, and spatially efficient. Chen et al. (2017) showed that adding 5% additives to microalgae during a mixed combustion efficiently removes NO_x; the additives reduced the amount of NO_x emission in the following order: $CuCl_2$ > SiC > $ZnCl_2$ > MgO. Ren et al. (2010) has shown a reduction in straw-N conversion into NH_3 and inhibition of N-conversion into HCN and HNCO by adding an iron additive, thereby reducing NO_x emission. During biomass combustion, the reduction in NO_x emissions can be influenced by the type and amount of additives at different temperatures. Therefore, it is important to identify the best additives and their optimal amounts at different temperatures.

This study reports the NO_x emission characteristics of fast-growing grass at different temperatures (600, 700, 750, 800, and 850°C), using varying mass fractions (3, 5, 10, and 15%) of different additives (Al_2O_3, CaO, $Ca(OH)_2$, and SiO_2). These results are expected to function as a reference to ensure the control of NO_x emission during the combustion of the fast-growing grass.

MATERIALS AND METHODS

Materials

The experimental samples were obtained from the fast-growing grass planting base in Yangshi Town, Loudi, Hunan. The industrial and elemental analyses of the grass are shown in **Table 1**. Analytical- and reagent-grade Al_2O_3, CaO, $Ca(OH)_2$, and SiO_2 with the purities of over 99, 98, 95, and 99%, respectively; all these are typical industrial additives that are applied to solid fuels. In this experiment, the following samples were tested: 1) samples of pure fast-growing grass; 2) mixture of fast-growing grass samples and additives at concentrations of 3, 5, 10, and 15%. All samples were pre-treated by drying in an electrothermal drying oven at 106°C for 12 h, followed by grinding and then sieving the particles through an 80-mesh sieve to obtain particles smaller than 200 μm in diameter. Finally, the samples were labelled and stored in dry containers for subsequent use.

Experimental Apparatus and Methods

The experimental system is illustrated in **Figure 1**. The combustion test was performed in a quartz tube reactor of a tube furnace with an inner diameter of 43 mm and a length of 600 mm (OTF-1200X, Hefei Kejing Material Technology Co., Ltd.). The temperature in the furnace was adjustable between room temperature and 1,200°C. NO_x emission was measured using a gas analyzer (Testo 350, Testo in Germany) connected to a computer that monitors and saves the experimental data in real time.

The experiment was performed using the following steps: 1) enter the target temperature into the temperature-control tube furnace and start heating; 2) open the gas cylinder valve and adjust N_2 and O_2 flowmeters such that their flows are 0.8 and 0.2 L/min, respectively; 3) after reaching the target temperature, weigh 0.2 g of each sample and spread it out in a porcelain boat; then, push the boat to the center of the tube furnace quickly; 4) place the probe of the gas analyzer at the gas outlet and observe the collected data on the computer. The combustion reaction was considered complete when the volume concentration of NO_x decreases to 2 ppm. Each set of experiments was repeated 3 times and average values were calculated.

Calculation Method

In this experiment, combustion is considered to be complete when the NO_x emission concentration falls to 2 ppm; the elapsed time is the burnout time t. Calculation formula references (Liu et al., 2018; Xu et al., 2021).

① The average concentration (AC) is calculated as follows:

$$AC = \frac{\int_0^t C dt}{t} \qquad (1)$$

Where, the numerator on the right-hand side refers to the integral of the gas concentration for the reaction time, t represents the burnout time, and the AC is measured in ppm.

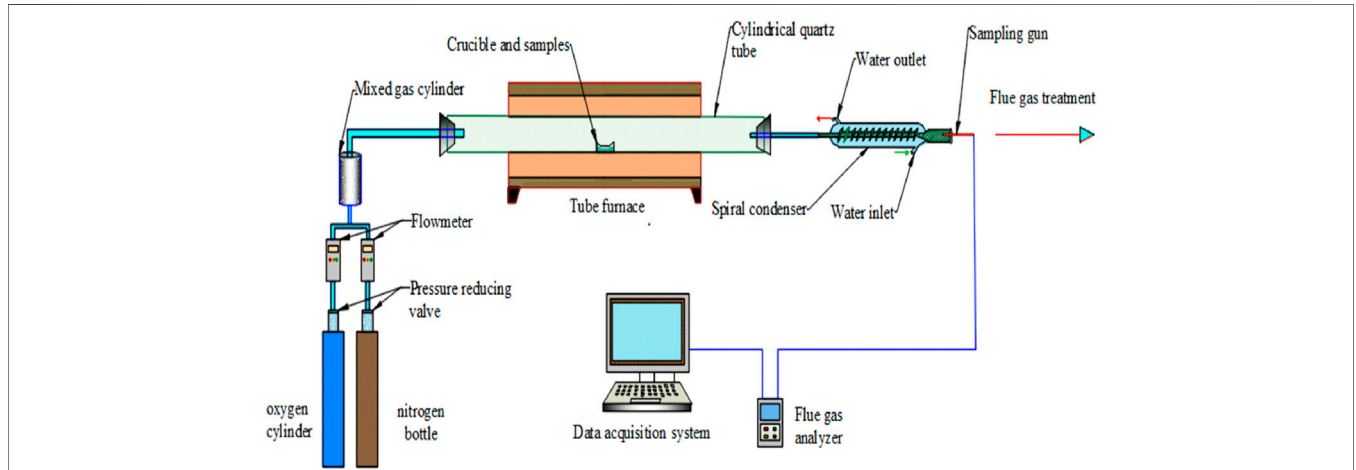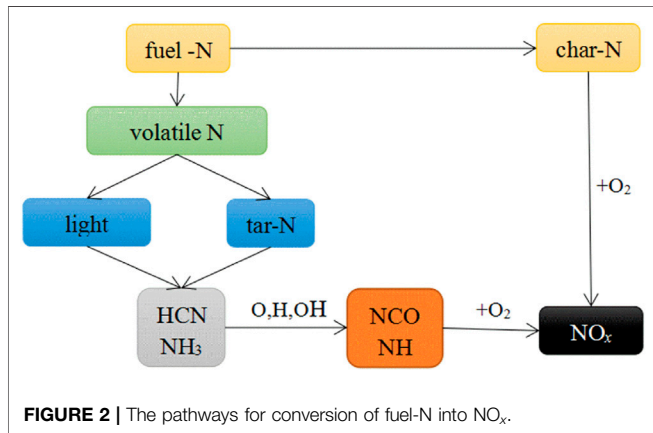| Fast-growing grass	Ultimate analysis						Proximate analysis		Calorific value (MJ/kg)
Aanalysis item	N	C	H	S	O	Ash content (A_d)	Volatile matter (V_d)	Fixed carbon (FC_d)	High calorific value ($Q_{gr,d}$)
Numerical value	0.730	40.102	5.241	0.260	46.107	7.56	78.88	13.56	18.20

FIGURE 1 | Experimental system.

FIGURE 2 | The pathways for conversion of fuel-N into NO_x.

② Calculation of NO_x volume (V)

Considering that the V is negligible compared to the input air volume, the V is approximately calculated as follows:

$$V = Q \times t \times \frac{AC}{10^6} \quad (2)$$

Where, the V is measured in L; Q represents the input air flow in L/s.

③ The mass (M) of produced NO_x is calculated as follows:

$$M = \frac{V \times 273.15}{T \times 22.4} \times M_g \quad (3)$$

Where, the unit of M is g; T(K) represents the temperature of the gas; M_g (g/mol) represents the molar mass of NO_x.

④ The denitration rate (η) is calculated as follows:

$$\eta = \frac{M_0 - M_1}{M_0} \times 100\% \quad (4)$$

Where, M_0 represents the mass of NO_x produced by combustion of samples without additives; M_1 is the mass of NO_x produced by combustion of samples with additives.

RESULTS AND DISCUSSION

The Effect of Temperature on NO_x Emission From Combustion of Fast-Growing Grass

The reaction pathway for NO_x generation by the oxidation of fuel-N (Vermeulen et al., 2012; Shah et al., 2019) shown in **Figure 2** displays that the following two main sources of NO_x in the flue gas: the conversion of volatile-N into volatile-NO_x; and the conversion of char-N into char-NO_x. The conversion of fuel-N mainly occurs at temperatures below 900°C; therefore, the NO_x emission levels were measured and analyzed in the flue gases from combustion of fast-growing grass at different temperatures below 900°C.

As shown in **Figure 3**, NO_x generated from volatile combustion appeared late (at 60s) in the NO_x emission curve at 600°C; the NO_x concentration (peak intensity) was rather low at 19.50 ppm and the combustion reaction lasted for 179 s. At a relatively low temperature of 600°C, not only is the volatilization slow, but the chemical reaction that generates volatile-NO_x from oxidation of volatile-N through intermediate products HCN and NH_3 is also extremely slow; therefore, NO_x concentration is

FIGURE 3 | NO_x release curves for fast-growing grass combustion at different temperatures.
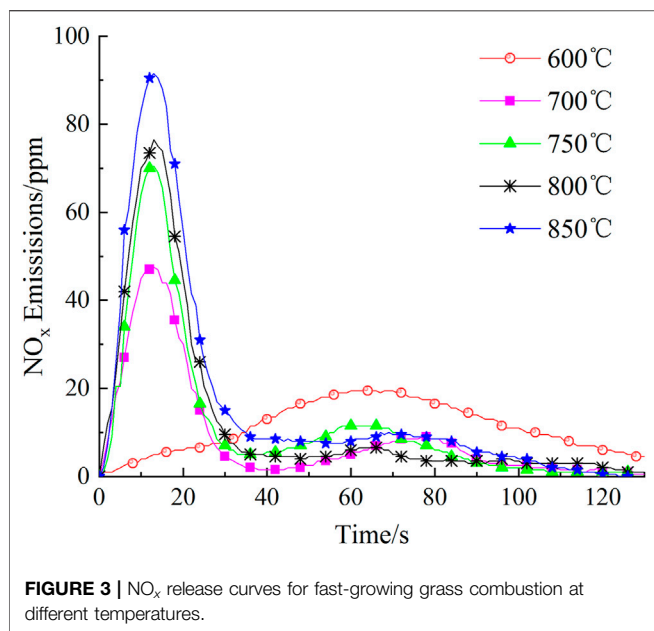
relatively low and the time of NO_x emission is rather long (Li et al., 2018; Shah et al., 2018). This is similar to that of microalgae combustion at 600℃ (Chen et al., 2017). Unlike at 600℃, two peaks were observed in the NO_x emission curves at 700, 750, 800, and 850℃, corresponding to the volatile and char combustion stages. At temperatures of 700, 750, 800, and 850℃, the first peak was observed much sooner at around 13 s; the peak intensities increased gradually as the temperature increased, reaching 47.50, 70.50, 76.50, and 91.50, respectively. This is similar to results observed for microalgae combustion (Sun et al., 2019; ZhaoSu, 2019), solid biomass combustion (LiChyang, 2020) and the mixed combustion of sewage sludge and rice husk (Xu et al., 2021b). The second peaks were observed in the NO_x emission curves at 77, 58, 62, and 67 s with intensities of 9.00, 11.50, 6.50, and 10.00 ppm, for 700, 750, 800, and 850℃, respectively; the intensities of these

peaks were much lower than those of the first peaks. Similar observations have also been reported in previous studies (Lane et al., 2013; Sun et al., 2019). These phenomena were attributed to the generation of char-NO_x from combustion of char-N of the fast-growing grass. The mechanism is shown in **Eq. 5** (Thomas et al., 1993; Molina et al., 2000; LI et al., 2007).

$$\text{char} - N + \frac{1}{2}O_2 \rightarrow NO \qquad (5)$$
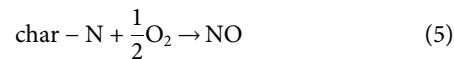
The Effects of a Additives on the NO_x Ggeneration From Combustion of the Fast-Growing Grass

Currently, NO_x removal is mainly achieved by adding additives to urea or ammonia solutions to introduce SNCR. However, these methods are damaging to the equipment and have high operating costs (Pudasainee et al., 2012); therefore, they are not applicable to small combustion equipment. Consequently, this study focused on mixed combustion of fast-growing grass along with additives to reduce NO_x emission at different combustion temperatures using varying mass fractions of four different additives.

Effects of Additives on Volatile-NO_x Generation

As shown in **Table 2**, the additives have an inhibitory effect on the generation of volatile-NO_x. At 600℃, the first peak of NO_x emission from combustion of fast-growing grass was significantly reduced after the introduction of additives. The peaks were reduced to average values of 34.40, 25.64, 16.01, 21.80% upon addition of SiO_2, Al_2O_3, CaO, and $Ca(OH)_2$, respectively. There are different reasons for the peak reduction for different additives. SiO_2 inhibits N-conversion to NO_x precursors (HCN, HNCO, and NH_3) during combustion (Ren et al., 2010); similarly, Al_2O_3 inhibits NO_x precursors generation

TABLE 2 | The first NO_x emission peaks from the combustion of fast-growing grass using different mass fractions of additives at 600℃.

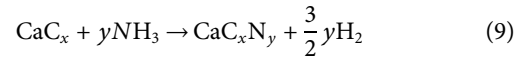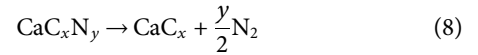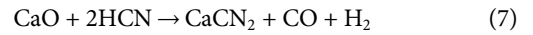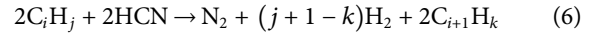| Temperature (℃)	Type of additive	Mass fraction	The first peak/ppm
600	Al_2O_3	Pure sample	19.50
		3%	13.50
		5%	14.50
		10%	15.00
		15%	15.00
	CaO	3%	16.50
		5%	15.67
		10%	16.67
		15%	16.67
	$Ca(OH)_2$	3%	17.00
		5%	12.50
		10%	15.00
		15%	16.50
	SiO_2	3%	13.00
		5%	11.00
		10%	11.67
		15%	15.50
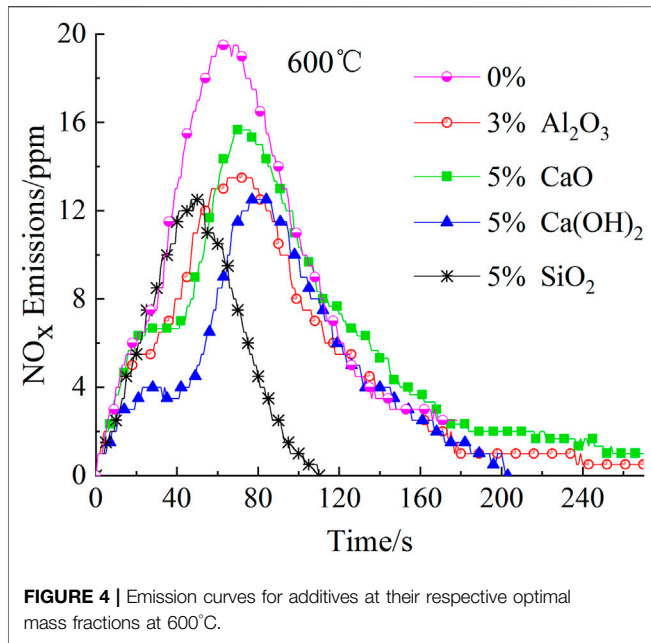
FIGURE 4 | Emission curves for additives at their respective optimal mass fractions at 600°C.

(Ren et al., 2010) and is often used as the carrier of the denitration catalyst (Ma. et al., 2015; Li et al., 2013; Yao et al., 2017; QiShan et al., 2020). On one hand, CaO can catalyze HCN to N_2, as shown in **Eq. 6** (Tan et al., 2009); on the other hand, it can also react with HCN and NH_3 to form N_2 during the pyrolysis stage, as shown in **Eqs. 7–9** (Fu et al., 2014; Liu et al., 2015; Zhang et al., 2017). Similarly, $Ca(OH)_2$ decomposes into CaO and H_2O at high temperatures exhibiting a peak-reducing effect, as shown in **Eq. 10** (Liu et al., 2015).

$$2C_iH_j + 2HCN \rightarrow N_2 + (j + 1 - k)H_2 + 2C_{i+1}H_k \quad (6)$$

$$CaO + 2HCN \rightarrow CaCN_2 + CO + H_2 \quad (7)$$

$$CaC_xN_y \rightarrow CaC_x + \frac{y}{2}N_2 \quad (8)$$

$$CaC_x + yNH_3 \rightarrow CaC_xN_y + \frac{3}{2}yH_2 \quad (9)$$

$$Ca(OH)_2 \rightarrow CaO + H_2O \quad (10)$$
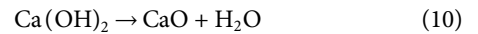
Surprisingly, just adding more additives did not have a better effect on reducing the peak. Optimal mass fractions were determined for the additives. For example, SiO_2, $Ca(OH)_2$, and CaO exhibited the best NO_x removal at a mass fraction of 5% with peak-reducing rates of 43.59, 35.90, and 19.64%, respectively. However, Al_2O_3 obtained the best reduction effect at a mass fraction of 3%, decreasing the peak intensity by 30.77%. These phenomena result from the agglomeration or blanketing of active components on the additive surface when the amount of additives reaches a

TABLE 3 | The first peak for NO_x emission from fast-growing grass combustion using different mass fractions of additives at different temperatures.

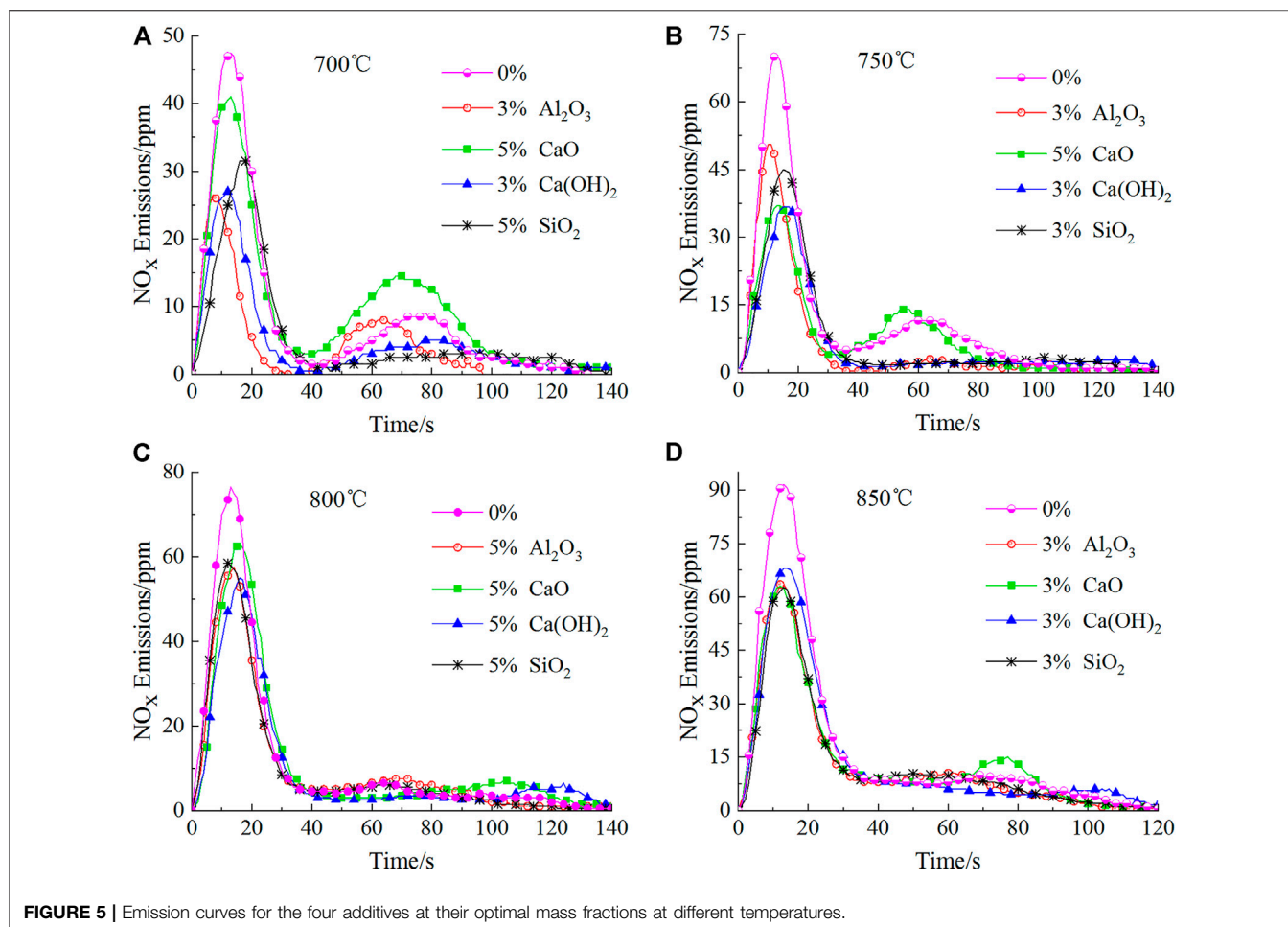| Temperature (°C)	Type of additive	Mass fraction	The first peak/ppm	Temperature (°C)	Type of additive	Mass fraction	The first peak/ppm
700	Al_2O_3	Pure sample	47.50	750	Al_2O_3	Pure sample	70.50
		3%	26.50			3%	50.50
		5%	27.50			5%	51.50
		10%	34.00			10%	55.50
		15%	32.00			15%	57.50
	CaO	3%	47.00		CaO	3%	43.50
		5%	41.00			5%	37.00
		10%	47.00			10%	44.00
		15%	43.50			15%	42.00
	$Ca(OH)_2$	3%	27.00		$Ca(OH)_2$	3%	36.67
		5%	29.00			5%	39.00
		10%	33.00			10%	43.00
		15%	28.67			15%	39.33
	SiO_2	3%	34.67		SiO_2	3%	45.00
		5%	31.50			5%	45.50
		10%	39.67			10%	48.67
		15%	38.50			15%	49.00
800	Al_2O_3	Pure sample	76.50	850	Al_2O_3	Pure sample	91.50
		3%	62.00			3%	63.50
		5%	57.50			5%	64.50
		10%	62.67			10%	73.00
		15%	58.00			15%	75.50
	CaO	3%	65.50		CaO	3%	63.00
		5%	63.00			5%	68.50
		10%	66.00			10%	75.33
		15%	63.00			15%	75.50
	$Ca(OH)_2$	3%	64.33		$Ca(OH)_2$	3%	68.00
		5%	55.00			5%	74.50
		10%	57.33			10%	75.00
		15%	56.67			15%	72.00
	SiO_2	3%	62.00		SiO_2	3%	62.67
		5%	58.50			5%	65.50
		10%	64.50			10%	77.50
		15%	64.00			15%	76.00

FIGURE 5 | Emission curves for the four additives at their optimal mass fractions at different temperatures.

certain value, which in -turn reduces of the number of active sites. Similar observations have also been reported by previous studies (Yu et al., 2017a; Sun et al., 2019). In order to further study the effects of additives on NO_x emission from the combustion of fast-growing grass at 600°C, the emission curves of the four additives at their optimal mass fractions (see **Figure 4**) were determined.

As shown in **Figure 4**, the additives affected not only the first peak of NO_x emission, but also its appearance time. The peak appeared 13 s sooner upon adding 5% SiO_2, whereas the peak appeared 16, 5, and 9 s later upon adding 5% $Ca(OH)_2$, 3% Al_2O_3, and 3% Al_2O_3, respectively. Similar phenomena have also been reported by Sun's research group (Sun et al., 2019).
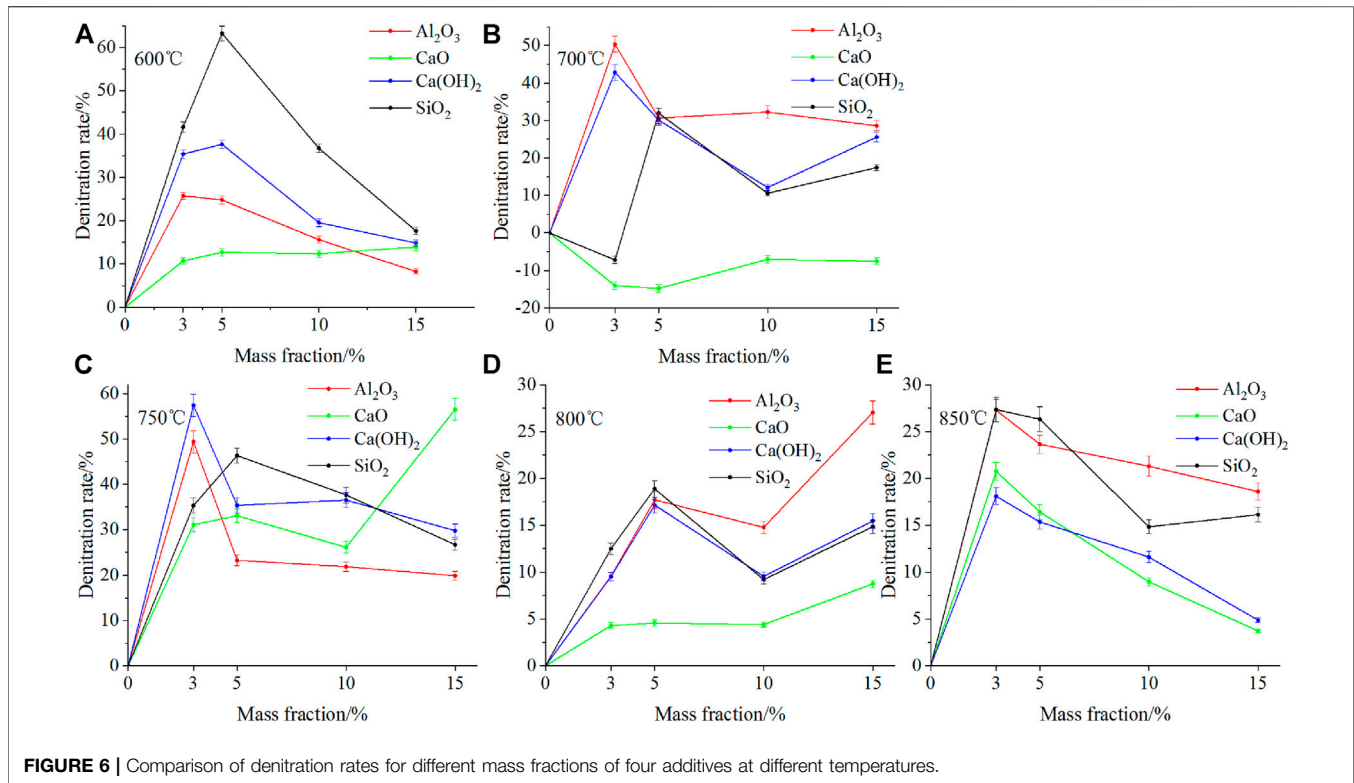
As the temperature changes, the effect of additives on lowering the first peak of NO_x emission varied, as shown in **Table 3**. Overall, at 700, 750, and 800°C, $Ca(OH)_2$ casued the most decrease in the first peak, whereas Al_2O_3 exhibited the same effect at 850°C. This is because of the relationship between the catalytic activity of the additives and the temperature (Sun et al., 2019), which caused the efficiency of NH_3 conversion to N_2 to differ at different temperatures.

Similar to the situation at 600°C, additives exhibited different rules to efficiently reduce the first peak at the same temperature,
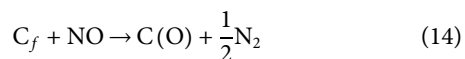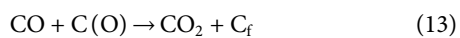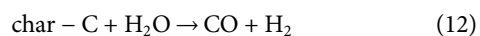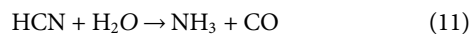
with varying mass fractions. For instance, at 700°C, Al_2O_3 and $Ca(OH)_2$ worked best at 3%, reducing the peak by 44.21 and 43.16%, respectively. At 800°C, however, Al_2O_3 and $Ca(OH)_2$ exhibited the best results at 5%, with the peak intensities dropping by 24.84 and 28.11%, respectively.

The Effects of Additives on the Generation of Char-NO_x

As shown in **Figure 5**, unlike the situation for 600°C, additives had little effect on the appearance time for the first peaks; the time for the peaks to appear was around 15 s after the addition of the four additives. However, the effect of different additives on the second peak varies, indicating that the additives have different effects on the production of char-NO_x. Al_2O_3 and SiO_2 reduced the second peak down to a certain extent, whose effect is unapparent in the high temperature zone (800°C and 850°C); however, it is quite obvious in the low temperature zone (700°C and 750°C). Unlike the two aforementioned additives, CaO increased the second peak to a certain extent, which is the most obvious at 700°C, and raised the second peak by 61.11% compared to that without additives. This may be because CaO can facilitate the conversion of char-N to char-NO_x (Liu et al., 2018b)

FIGURE 6 | Comparison of denitration rates for different mass fractions of four additives at different temperatures.

and function most efficiently at 700°C (HayhurstLawrence, 1996). These phenomena will be further investigated in subsequent studies. Interestingly, the situation of $Ca(OH)_2$ is opposite to that of CaO. It all depends on whether the H_2O generated after decomposition of $Ca(OH)_2$ reacts with the HCN and char-C to produce CO, the reaction mechanism for which is shown in **Eq. 11** (Liu et al., 2017; SchäferBonn, 2002) and **Eq. 12** (Heikkilä et al., 2021; HermannHüttinger, 1986; MoulijnKapteijn, 1995); it also matters whether CO can convert NO to N_2, whose reaction mechanism is shown in **Eq. 13, 14** (Chan et al., 1983; Thomas et al., 1993; AarnaSuuberg, 1997; Dong et al., 2007; Gong et al., 2021).

$$HCN + H_2O \rightarrow NH_3 + CO \qquad (11)$$

$$char - C + H_2O \rightarrow CO + H_2 \qquad (12)$$

$$CO + C(O) \rightarrow CO_2 + C_f \qquad (13)$$

$$C_f + NO \rightarrow C(O) + \frac{1}{2}N_2 \qquad (14)$$

The Effect of Additives on the Denitration Rate for Combustion of the Fast-Growing Grass

Figure 6 presents the denitration rate for the combustion of fast-growing grass with four mass fractions of four different additives at different temperatures. As shown in **Figure 6**, at different temperatures, four additives exhibited different NO_x removal effects. At 600 and 750°C, SiO_2 and CaO displayed the best

denitration effects with average denitration rates of 39.80 and 42.69%, respectively. At 700, 800, and 850°C, Al_2O_3 demonstrated the best denitration effect with average denitration rates of 34.56, 17.27, and 22.71%, respectively, The denitrification effect is better than $CaCO_3$ (Qi et al., 2017)and calcium and Ca-Fe oxides additives (Yu et al., 2017b; Qi et al., 2017). The addition of CaO at 700°C showed no denitrification effect and the average yield of NO_x increased by 10.86%, this is because it promotes the production of char-NO_x.

As shown in **Figure 6**, at the same temperature, the same additive displayed different NO_x removal effects (η) for different mass fractions. At 600 °C, $Ca(OH)_2$ worked best (η = 63.28%) at a mass fraction of 5%; at 700°C, Al_2O_3 showed the best effect (η = 50.34%) at 3%, whereas CaO failed to make any difference but rather increased NO_x emission; at 750°C, $Ca(OH)_2$ worked (η = 57.44%) the best at a mass fraction of 3%; at 800°C, Al_2O_3 worked best (η = 27.05%) at a mass fraction of 15%; at 850°C, Al_2O_3 worked best (η = 27.28%) at a mass fraction of 3%.

According to the peak-reducing effect and NO_x removal effect of the additives on NO_x emission from the combustion of fast-growing grass, the optimal control conditions at different temperatures are as follows: 1) at 600°C, 5% SiO_2 is the best, with the highest peak-reducing rate and NO_x removal efficiency; 2) at 700 and 750°C, 3% Al_2O_3 and 3% $Ca(OH)_2$ are the best, respectively; 3) at 800°C, 5% $Ca(OH)_2$ has the best peak-reducing effect; however, it has a much lower (9.89% lower) NO_x removal efficiency than that of 15% Al_2O_3; 15% Al_2O_3 has the highest NO_x removal efficiency with a slightly lower (3.92% lower) peak-reducing effect than that of 5% $Ca(OH)_2$; therefore, at 800°C, 15% Al_2O_3 is the best; 4) at 850°C, 3% SiO_2 and

3% Al_2O_3 are better and acceptable, with a gap of only 0.91% in the peak-reducing effect and only 0.06% in the NO_x removal efficiency.

CONCLUSIONS

The temperature one of the most critical influences on NO_x emission from the fast-growing grass combustion. As the combustion temperature rises, the average concentration of NO_x emission from the combustion of fast-growing grass increases. which agrees with the law of NO_x emission in biomass combustion. Moreover, at 700, 750, 800, and 850°C, the second peaks were found to be much lower than the first peaks of NO_x emission.

The type and mass fraction of additives also have an important impact on the NO_x emission. Additives can inhibit the formation of volatile-NO_x and also influence the production of char-NO_x to varying degrees. In particular, different from the other three additives, CaO can promote the production of char-NO_x. At the same temperature, different additives have their respective optimal mass fractions to reduce NO_x emission.

In addition, the type and mass fraction of additives affect the denitration rate of combustion of the fast-growing grass. The best additive and its optimal mass fraction vary at different temperatures. Considering both the peaks of NO_x emission and NO_x removal efficiencies at experimental temperatures, the optimal controlling conditions for NO_x emission were obtained. The research results can serve as data reference for NO_x emission control during the combustion of the fast-growing grass.

REFERENCES

Aarna, I., and Suuberg, E. M. (1997). A Review of the Kinetics of the Nitric Oxide-Carbon Reaction. *Fuel.* 76 (6), 475–491. doi:10.1016/S0016-2361(96)00212-8

Bae, S. W., Roh, S. A., and Kim, S. D. (2006). NO Removal by Reducing Agents and Additives in the Selective Non-Catalytic Reduction (SNCR) Process. *Chemosphere.* 65 (1), 170–175. doi:10.1016/j.chemosphere.2006.02.040

Cai, J., Zheng, W., and Wang, Q. (2021). Effects of Hydrogen Peroxide, Sodium Carbonate, and Ethanol Additives on the Urea-Based SNCR Process. *Sci. Total Environ.* 772, 145551. doi:10.1016/j.scitotenv.2021.145551

Chan, L. K., Sarofim, A. F., and Beér, J. M. (1983). Kinetics of the NO carbon Reaction at Fluidized Bed Combustor Conditions. *Combustion and Flame* 52, 37–45. doi:10.1016/0010-2180(83)90119-0

Chen, C., Chen, F., Cheng, Z., Chan, Q. N., Kook, S., and Yeoh, G. H. (2017). Emissions Characteristics of NO_X and SO_2 in the Combustion of Microalgae Biomass Using a Tube Furnace. *J. Energ. Inst.* 90 (5), 806–812. doi:10.1016/j.joei.2016.06.003

Chen, H., Chen, D. Z., Fan, S., Hong, L., and Wang, D. (2016). SNCR De-NO X Within a Moderate Temperature Range Using Urea-Spiked Hydrazine Hydrate as Reductant. *Chemosphere.* 161, 208–218. doi:10.1016/j.chemosphere.2016.07.010

Dong, L., Gao, S., Song, W., and Xu, G. (2007). Experimental Study of NO Reduction Over Biomass Char. *Fuel Process. Technol.* 88 (7), 707–715. doi:10.1016/j.fuproc.2007.02.005

Fu, S.-l., Song, Q., Tang, J.-s., and Yao, Q. (2014). Effect of CaO on the Selective Non-Catalytic Reduction DeNO Process: Experimental and Kinetic Study. *Chem. Eng. J.* 249, 252–259. doi:10.1016/j.cej.2014.03.102

Gasnot, L., Dao, D. Q., and Pauwels, J. F. (2012). Experimental and Kinetic Study of the Effect of Additives on the Ammonia Based SNCR Process in Low Temperature Conditions. *Energy Fuels.* 26 (5), 2837–2849. doi:10.1021/ef300310c

Gong, Q.-C., He, L.-Q., Zhang, L.-H., and Duan, F. (2021). Comparison of the NO Heterogeneous Reduction Characteristics Using Biochars Derived from Three

DATA AVAILABILITY STATEMENT

The original contributions presented in the study are included in the article/**Supplementary Material**, further inquiries can be directed to the corresponding author.

AUTHOR CONTRIBUTIONS

HL: paper writing. QH: experiments. HL: supervisor. ZH: evaluation of results. XZ: experiments. WC: technical support. XZ: evaluation of results. SP: technical support. All authors: contributed to the article and approved the submitted version.

FUNDING

SUPPLEMENTARY MATERIAL

The Supplementary Material for this article can be found online at: https://www.frontiersin.org/articles/10.3389/fenrg.2021.772755/full#supplementary-material.

Biomass With Different Lignin Types. *J. Environ. Chem. Eng.* 9 (1), 105020. doi:10.1016/j.jece.2020.105020

Hao, J., Yu, W., Lu, P., Zhang, Y., and Zhu, X. (2015). The Effects of Na/K Additives and Flyash on NO Reduction in a SNCR Process. *Chemosphere.* 122, 213–218. doi:10.1016/j.chemosphere.2014.11.055

Hayhurst, A. N., and Lawrence, A. D. (1996). The Effect of Solid CaO on the Production of NO_x and N_2O in Fluidized Bed Combustors: Studies Using Pyridine as a Prototypical Nitrogenous Fuel. *Combustion and Flame.* 105 (4), 511–527. doi:10.1016/0010-2180(95)00219-7

Heikkilä, A. M., Koskela, A. M., Iljana, M. O., Lin, R., Bartusch, H., Heikkinen, E.-P., et al. (2021). Coke Gasification in Blast Furnace Shaft Conditions With H_2 and H_2O Containing Atmospheres. *Steel Research Int.* 92 (3), 2000456. doi:10.1002/srin.202000456

Hermann, G., and Hüttinger, K. J. (1986). Mechanisms of Non-Catalysed and Iron-Catalysed Water Vapour Gasification of Carbon. *Fuel.* 65 (10), 1410–1418. doi:10.1016/0016-2361(86)90115-8

Lane, D. J., Ashman, P. J., Zevenhoven, M., Hupa, M., van Eyk, P. J., de Nys, R., et al. (2013). Combustion Behavior of Algal Biomass: Carbon Release, Nitrogen Release, and Char Reactivity. *Energy Fuels.* 28 (1), 41–51. doi:10.1021/ef4014983

Lee, S., Park, K., Park, J., and Kim, B. (2005). Characteristics of Reducing NO Using Urea and Alkaline Additives. *Combustion and flame.* 141 (3), 200–203. doi:10.1016/j.combustflame.2005.01.004

Lei, X. (2015). Carbon Sink Grass and its Carbon Sink Mechanism. *Agric. Eng. (Chinese)* 5 (5), 38–43. doi:10.3969/j.issn.2095-1795.2015.05.014

Lei, X. (2017). Comprehensively Carry Out General Secretary Xi Jinping's Important Strategic Thought on Ecological Civilization Construction. *Energy China (Chinese)* 39 (7), 4–11. doi:10.3969/j.issn.1003-2355.2017.07.001

Li, P.-W., and Chyang, C.-S. (2020). A Comprehensive Study on NOx Emission and Fuel Nitrogen Conversion of Solid Biomass in Bubbling Fluidized Beds Under Staged Combustion. *J. Energ. Inst.* 93 (1), 324–334. doi:10.1016/j.joei.2019.02.007

Li, P.-W., Chyang, C.-S., and Ni, H.-W. (2018). An Experimental Study of the Effect of Nitrogen Origin on the Formation and Reduction of NOx in Fluidized-Bed Combustion. *Energy.* 154, 319–327. doi:10.1016/j.energy.2018.04.141

Li, P., Li, J., Hu, Y., Wan, Y., Yue, Y., Jing, Z., Hu, N., Yang, J., and Yang, G. (2007). "*Research On NO$_X$ Emission Characteistics And Mechanism during Sewage Sludge/Coal Mixtures Combustion,*" in Proceeding of the International symposium on coal combustion, Wuhan(CN).

Li, R. H., Zhou, S., Li, C. L., Wang, Z. Y., and Zhu, Y. Q. (2013). A Study on SCR Catalyst Support. *Adv. Mater. Res.* 726-731, 17–20. doi:10.4028/www.scientific.net/AMR.726-731.17

Liu, H., Yi, L., Hu, H., Xu, K., Zhang, Q., Lu, G., et al. (2017). Emission Control of NO$_X$ Precursors During Sewage Sludge Pyrolysis Using an Integrated Pretreatment of Fenton Peroxidation and CaO Conditioning. *Fuel.* 195, 208–216. doi:10.1016/j.fuel.2017.01.067

Liu, H., Zhang, Q., Hu, H., Liu, P., Hu, X., Li, A., et al. (2015). Catalytic Role of Conditioner CaO in Nitrogen Transformation During Sewage Sludge Pyrolysis. *Proc. Combustion Inst.* 35 (3), 2759–2766. doi:10.1016/j.proci.2014.06.034

Liu, X., Luo, Z., and Yu, C. (2018a). Effect of limestone on the Emission of NO during Petroleum Coke Combustion. *Fuel.* 224, 1–9. doi:10.1016/j.fuel.2018.03.066

Liu, X., Luo, Z., and Yu, C. (2018b). Effect of limestone on the Emission of NO During Petroleum Coke Combustion. *Fuel.* 224, 1–9. doi:10.1016/j.fuel.2018.03.066

Ma, L., Qi, Y. F., Wang, M. T., and Li, Z. M. (2015). "Investigation of Micro-characteristics on Manganese-Basis Catalysts for Denitration Prepared by Different Carriers," in International conference on computer science and environmental engineering(CSEE 2015), Beijing, China, May-2015, 172–178.

Molina, A., Eddings, E. G., Pershing, D. W., and Sarofim, A. F. (2000). Char Nitrogen Conversion: Implications to Emissions from Coal-Fired Utility Boilers. *Prog. Energ. combustion Sci.* 26 (4), 507–531. doi:10.1016/S0360-1285(00)00010-1

Moulijn, J. A., and Kapteijn, F. (1995). Towards a Unified Theory of Reactions of Carbon with Oxygen-Containing Molecules. *Carbon.* 33 (8), 1155–1165. doi:10.1016/0008-6223(95)00070-T

National Joint Center for air pollution control (2019). Nitrate Has Become the Most Important Secondary Inorganic Component in PM2.5 in Beijing, Tianjin and Hebei 03/15, 2021. Available at: https://huanbao.bjx.com.cn/news/20190313/968481.shtml.

Niu, S., Han, K., and Lu, C. (2010). Experimental Study on the Effect of Urea and Additive Injection for Controlling Nitrogen Oxides Emissions. *Environ. Eng. Sci.* 27 (1), 47–53. doi:10.1089/ees.2008.0181

Pudasainee, D., Kim, J.-H., Yoon, Y.-S., and Seo, Y.-C. (2012). Oxidation, Reemission and Mass Distribution of Mercury in Bituminous Coal-Fired Power Plants With SCR, CS-ESP and Wet FGD. *Fuel.* 93, 312–318. doi:10.1016/j.fuel.2011.10.012

Qi, J., Han, K., Wang, Q., and Gao, J. (2017). Carbonization of Biomass: Effect of Additives on Alkali Metals Residue, SO 2 and NO Emission of Chars during Combustion. *Energy* 130, 560–569. doi:10.1016/j.energy.2017.04.109

Qi, Y., Ge, P., Wang, M., Shan, X., Ma, R., Huang, J., et al. (2020a). Experimental Investigation and Numerical Simulation of Simultaneous Desulfurization and Denitrification by H$_2$O$_2$ Solution Assisted With Microwave and Additive. *Chem. Eng. J.* 391, 123559. doi:10.1016/j.cej.2019.123559

Qi, Y., Shan, X., Wang, M., Hu, D., Song, Y., Ge, P., et al. (2020b). Study on Low-Temperature SCR Denitration Mechanisms of Manganese-Based Catalysts With Different Carriers. *Water Air Soil Pollut.* 231 (6), 289. doi:10.1007/s11270-020-04644-5

Recalde, M., Woudstra, T., and Aravind, P. V. (2019). Gasifier, Solid Oxide Fuel Cell Integrated Systems for Energy Production From Wet Biomass. *Front. Energ. Res.* 7, 129. doi:10.3389/fenrg.2019.00129

Ren, Q., Zhao, C., Wu, X., Liang, C., Chen, X., Shen, J., et al. (2010). Catalytic Effects of Fe, Al and Si on the Formation of NOX Precursors and HCl during Straw Pyrolysis. *J. Therm. Anal. Calorim.* 99 (1), 301–306. doi:10.1007/s10973-009-0150-0

Rota, R., and Zanoelo, E. F. (2003). Influence of Oxygenated Additives on the NOxOUT Process Efficiency☆. *Fuel.* 82 (7), 765–770. doi:10.1016/S0016-2361(02)00365-4

Schäfer, S., and Bonn, B. (2002). Hydrolysis of HCN as an Important Step in Nitrogen Oxide Formation in Fluidised Combustion. Part II: Heterogeneous Reactions Involving limestone. *Fuel.* 81 (13), 1641–1646. doi:10.1016/S0016-2361(02)00096-0

Shah, I. A., Gou, X., and Wu, J. (2019). Simulation Study of an Oxy-Biomass-Based Boiler for Nearly Zero Emission Using Aspen Plus. *Energies.* 12 (10), 1949. doi:10.3390/en12101949

Shah, I. A., Gou, X., Zhang, Q., Wu, J., Wang, E., and Liu, Y. (2018). Experimental Study on NOx Emission Characteristics of Oxy-Biomass Combustion. *J. Clean. Prod.* 199, 400–410. doi:10.1016/j.jclepro.2018.07.022

Sun, J., Zhao, B., and Su, Y. (2019). Advanced Control of NO Emission from Algal Biomass Combustion Using Loaded Iron-Based Additives. *Energy.* 185, 229–238. doi:10.1016/j.energy.2019.07.042

Tan, H., Wang, X., Wang, C., and Xu, T. (2009). Characteristics of HCN Removal Using CaO at High Temperatures. *Energy Fuels.* 23 (2), 1545–1550. doi:10.1021/ef800935u

Thomas, K. M., Grant, K., and Tate, K. (1993). Nitrogen-Doped Carbon-13 Materials as Models for the Release of NOx and N$_2$O during Coal Char Combustion. *Fuel.* 72 (7), 941–947. doi:10.1016/0016-2361(93)90291-9

Vermeulen, I., Block, C., and Vandecasteele, C. (2012). Estimation of Fuel-Nitrogen Oxide Emissions from the Element Composition of the Solid or Waste Fuel. *Fuel.* 94, 75–80. doi:10.1016/j.fuel.2011.11.071

Wang, F., Chen, T., Jin, M., and Lu, P. (2014). Simultaneous Desulfurization and Denitrification from Flue Gas Using Urea/Piperazine Solution. *Adv. Mater. Res.* 881-883 (1764), 641–644. doi:10.4028/www.scientific.net/AMR.881-883.641

Wang, K., Khoo, K. S., Chew, K. W., Selvarajoo, A., Chen, W.-H., Chang, J.-S., et al. (2021). Microalgae: The Future Supply House of Biohydrogen and Biogas. *Front. Energ. Res.* 9, 660399. doi:10.3389/fenrg.2021.660399

Wang, Q., Han, K., Wang, P., Li, S., and Zhang, M. (2020). Influence of Additive on Ash and Combustion Characteristics During Biomass Combustion under O2/CO2 Atmosphere. *Energy.* 195, 116987. doi:10.1016/j.energy.2020.116987

Xiaorui, L., Xudong, Y., Guilin, X., and Yiming, Y. (2021). NO Emission Characteristic During Fluidized Combustion of Biomass With Limestone Addition. *Fuel.* 291, 120264. doi:10.1016/j.fuel.2021.120264

Xu, G., Ou, J., Fang, B., Wei, H., Hu, T., and Wang, H. (2021a). NO Emission From the Combustion of Mixed Fuel Pellets of Fenton/CaO-Conditioned Municipal Sludge and Rice Husk. *Environ. Pollut.* 281, 117018. doi:10.1016/j.envpol.2021.117018

Xu, G., Ou, J., Fang, B., Wei, H., Hu, T., and Wang, H. (2021b). NO Emission From the Combustion of Mixed Fuel Pellets of Fenton/CaO-Conditioned Municipal Sludge and rice Husk. *Environ. Pollut.* 281, 117018. doi:10.1016/j.envpol.2021.117018

Xu, Q., Wang, S., Jiang, J., Bhattarai, N., Li, X., Chang, X., et al. (2019). Nitrate Dominates the Chemical Composition of PM2.5 during Haze Event in Beijing, China. *Sci. Total Environ.* 689, 1293–1303. doi:10.1016/j.scitotenv.2019.06.294

Yao, X., Kong, T., Yu, S., Li, L., Yang, F., and Dong, L. (2017). Influence of Different Supports on the Physicochemical Properties and Denitration Performance of the Supported Mn-Based Catalysts for NH3-SCR at Low Temperature. *Appl. Surf. Sci.* 402, 208–217. doi:10.1016/j.apsusc.2017.01.081

Yu, Z.-y., Fan, X.-h., Gan, M., and Chen, X.-l. (2017a). Effect of Ca-Fe Oxides Additives on NOx Reduction in Iron Ore Sintering. *J. Iron Steel Res. Int.* 24 (12), 1184–1189. doi:10.1016/S1006-706X(18)30016-5

Yu, Z.-y., Fan, X.-h., Gan, M., and Chen, X.-l. (2017b). Effect of Ca-Fe Oxides Additives on NOx Reduction in Iron Ore Sintering. *J. Iron Steel Res. Int.* 24 (12), 1184–1189. doi:10.1016/S1006-706X(18)30016-5

Zhang, Q., Liu, H., Lu, G., Yi, L., Hu, H., Chi, H., et al. (2017). Mechanism of Conditioner CaO on NOx Precursors Evolution During Sludge Steam Gasification. *Proc. Combustion Inst.* 36 (3), 4003–4010. doi:10.1016/j.proci.2016.09.006

Zhao, B., and Su, Y. (2019). Emission and Conversion of NO From Algal Biomass Combustion in O2/CO2 Atmosphere. *J. Environ. Manage.* 250, 109419. doi:10.1016/j.jenvman.2019.109419